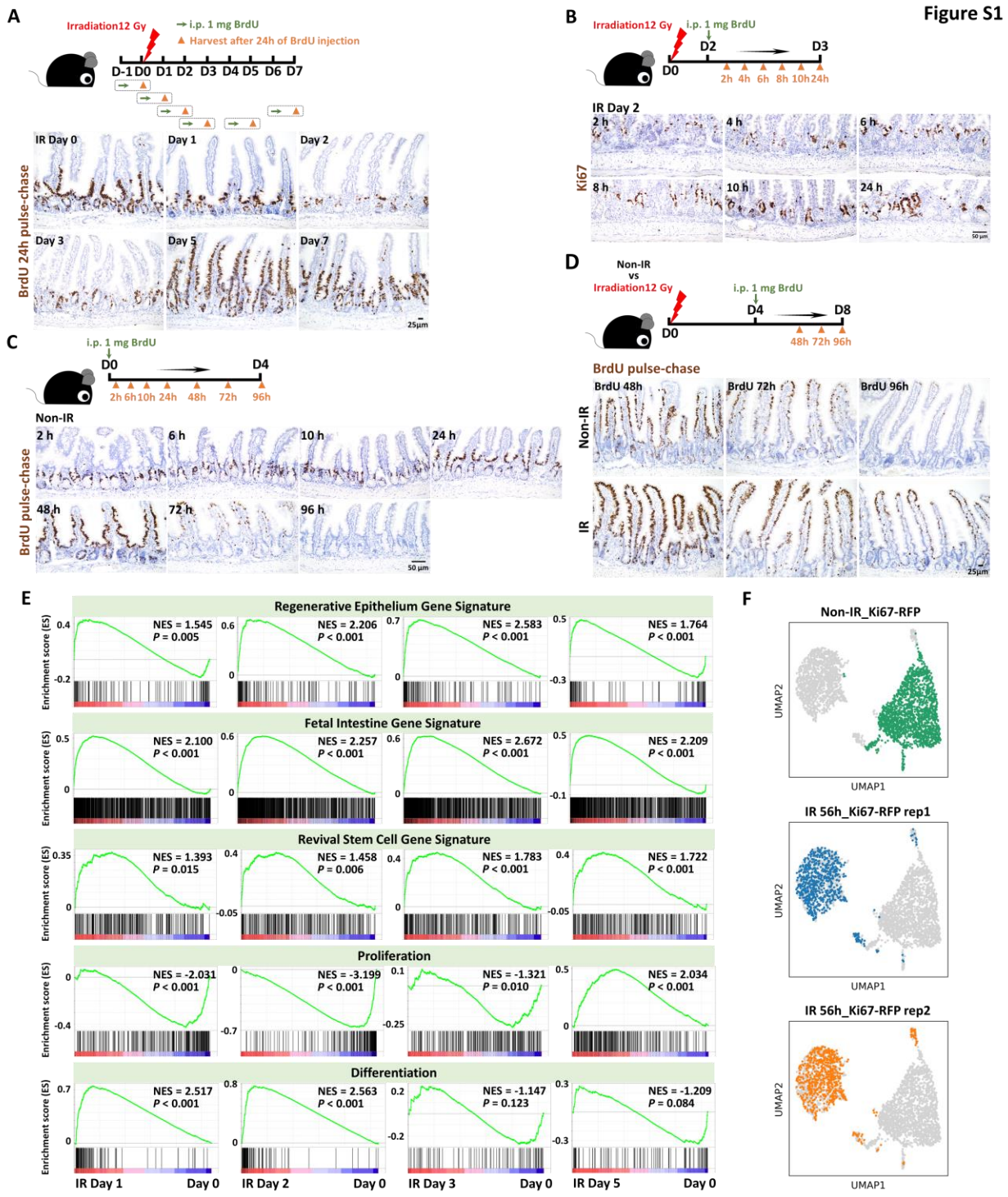

Figure S1. Day 2 to Day 3 post-irradiation is a critical regeneration period of crypt cells. (A) BrdU pulse-chase immunostaining of the intestine upon irradiation (representative of 3 biological replicates). Mice were injected with 1 mg of BrdU before or after irradiation. Intestines were collected after 24 hours of BrdU injection (see time-course details in the schematic of experimental design). **(B)** Immunostaining of Ki67 in the intestinal tissues of mice after 12 Gy irradiation. Ki67: proliferative marker, brown color; representative of 3 biological replicates. The schematic of experimental design was the same as BrdU

experiment performed in **Figure 1B**. **(C)** BrdU pulse-chase immunostaining of the intestinal tissues collected from the non-IR control mice (representative of 3 biological replicates). For BrdU immunohistochemistry, mice were injected with 1 mg of BrdU. Intestinal tissues were harvested after 2, 6, 10, 24, 48, 72 and 96 hours of BrdU injection. **(D)** BrdU pulse-chase immunostaining of the intestinal tissues (representative of 3 biological replicates). Mice were injected with 1 mg of BrdU at Day 4 post-irradiation. Tissues were collected after 48, 72 and 96 hours of BrdU injection (see time-course details in the schematic of experimental design). BrdU positive cells are marked brown. Non-IR mice were used as controls. **(E)** GSEA examines expression changes in gene signatures of regenerative epithelium, fetal spheroid, revival stem cell, proliferation, and differentiation (Ayyaz et al., 2019; Merlos-Suarez et al., 2011; Mustata et al., 2013; Wang et al., 2019; Yui et al., 2018) at time points post-irradiation. Bulk RNA-seq was used in this analysis (GSE165157 (Qu et al., 2021), crypt cells, n=2 biological replicates per time-course, Kolmogorov-Smirnov test). **(F)** scRNA-seq reveals that sorted Ki67-RFP positive cells show different transcriptome profiles after 56 hours of irradiation compared to the non-IR controls. Number of cells in each condition was Non-IR Ki67-RFP positive cells: n=1739; IR 56h Ki67-RFP positive cells replicate 1: n=677; IR 56h Ki67-RFP positive cells replicate 2: n= 669. Ki67-RFP positive cells were isolated and sorted from crypt cells of *Mki67tm1.1Cle/J* mice after 56 hours of IR vs. non-IR control.

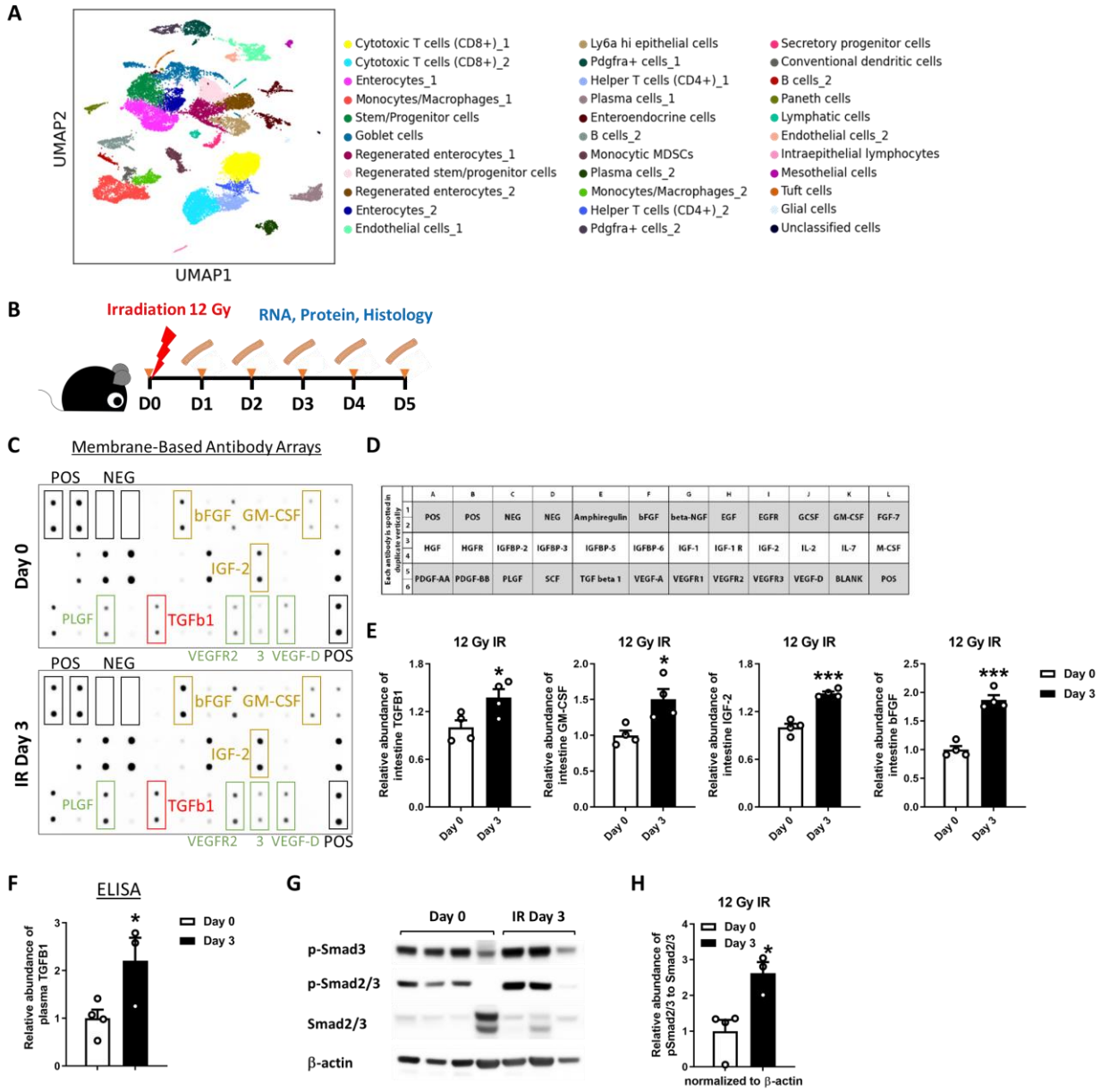

	A	B	C	D	E	F	G	H	I	J	K	L
Each antibody is spotted in duplicate vertically	POS	POS	NEG	NEG	Amphiregulin	bFGF	beta-NGF	EGF	EGFR	GCSF	GM-CSF	FGF-7
	HGF	HGFR	IGFBP-2	IGFBP-3	IGFBP-5	IGFBP-6	IGF-1	IGF-1 R	IGF-2	IL-2	IL-7	M-CSF
	PDGF-AA	PDGF-BB	PLGF	SCF	TGF beta 1	VEGF-A	VEGFR1	VEGFR2	VEGFR3	VEGF-D	BLANK	POS

Figure S2. TGFB signaling is activated in Day 3 irradiated mouse intestine. (A) Identified cell populations of intestinal scRNA-seq data following mouse irradiation at days 0, 1, 3, 7, and 14, as shown in **Figure 2B** (GSE165318, n=3-4 biological replicates per time-course). **(B)** Schematics of IR time-course and sample collection for RNA, protein and histology. **(C-E)** IGF-2 is reported to preprogram maturing macrophages (TGFB1 producers) to acquire oxidative phosphorylation-dependent anti-inflammatory properties (Du et al., 2019). On the other hand, TGFB1 is known to enhance CM-CSF (Celada and Maki, 1992) and bFGF (Pertovaara et al., 1993), and we found TGFB1 and its related growth factors are all enriched in Day 3 intestine post-irradiation. Increased PLGF and VEGF were reported under pathologic situations, which are also observed in our study. **(E)** Quantification (n=2 independent experiments, 2 technical replicates per membrane, Student's t-test at $P < 0.001$*** and $P < 0.05$*). **(F)** Increased TGFB1 is observed in plasma at Day 3 post-irradiation compared to Day 0, as determined by ELISA (n=3-4

biological replicates, Student's t-test at $P < 0.05$*). **(G-H)** Western blot reveals that increased p-Smad3 and p-Smad2/3 levels (TGFB pathway) are detected in the intestine after 3 days of irradiation. **(H)** Quantification of western blot (n=3-4 biological replicates, Student's t-test at $P < 0.05$*). TGFB1: Transforming growth factor beta 1; bFGF: Basic fibroblast growth factor; GM-CSF: Granulocyte-macrophage colony-stimulating factor; IGF-2: insulin-like growth factor; PLGF: Placental growth factor; VEGF: Vascular endothelial growth factor.

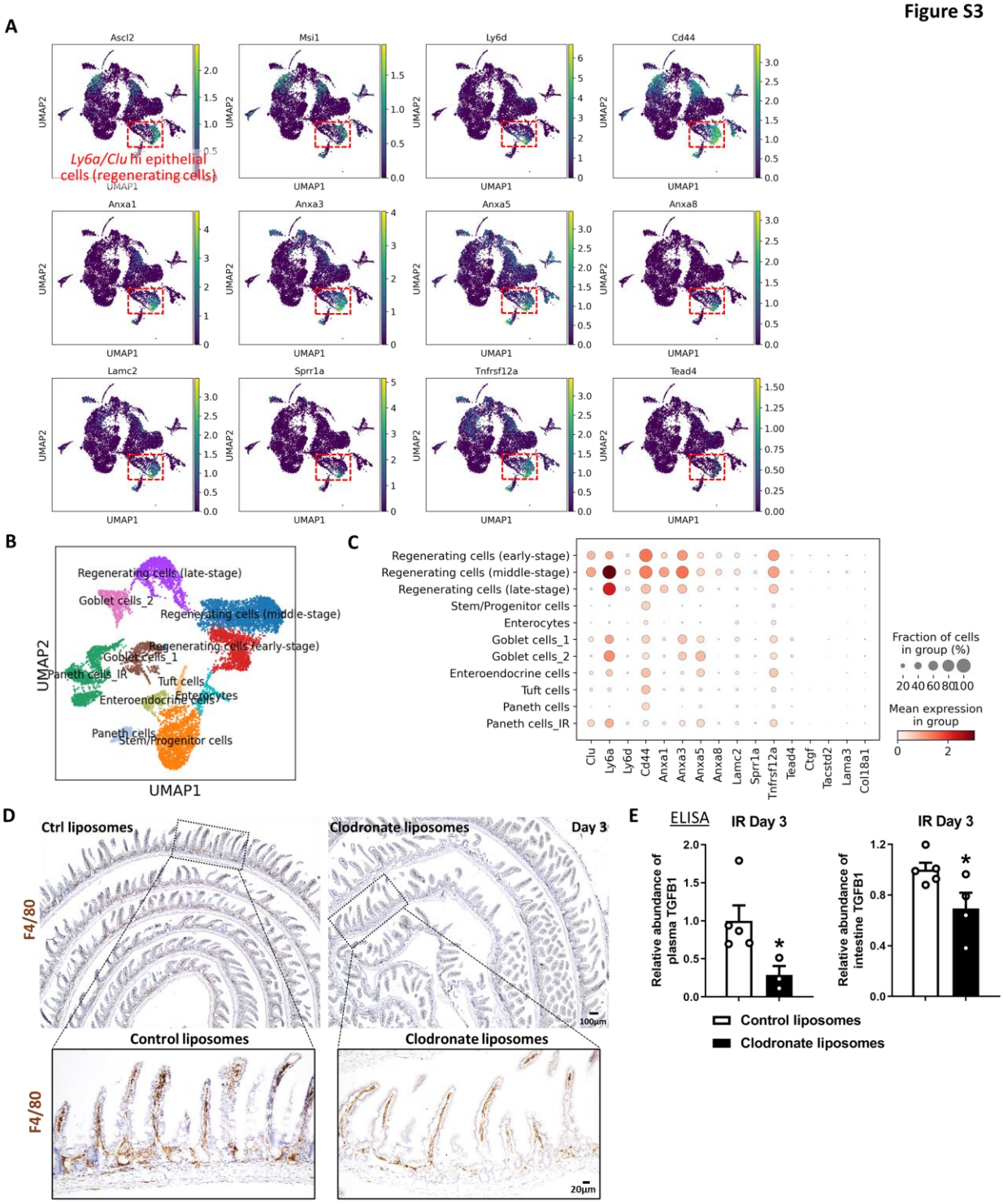

Figure S3. Fetal/regenerative genes are highly enriched during regeneration. (A) scRNA-seq of mouse intestines across a time-course post-irradiation (GSE165318). Of all the epithelial cells in the dataset (marked by *Epcam* expression in **Figure 3B**), regenerating cells expressing *Tgfbr2* are also highly enriched in transcript levels of reserve stem cell genes and fetal/regenerative marker genes. **(B-C)** *Msi1-CreERT2; R26-mTmG* mice were treated with tamoxifen for 15 hours, and *Msi1* positive GFP cells were sorted for

scRNA-seq. Identified cell populations **(B)** of intestinal scRNA-seq data following mouse irradiation at days 0, 1, 2, 3, and 5 (GSE145866 (Sheng et al., 2020)). Fetal/regenerative transcripts **(C)** are highly enriched in these regenerating cells. **(D-E)** Monocytes/Macrophages were depleted using clodronate-containing liposomes (see schematic of experimental design in **Figure 3F**). Immunostaining **(D)** was performed to confirm reduction in F4/80 (monocyte/macrophage marker) expressing cells upon treatment. Reduced levels of TGFB1 are observed in the plasma and intestine upon treatment of clodronate liposomes compared to treatment with control liposomes, as evidenced by ELISA **(E)**. Plasma and duodenal fragments were collected 3 days post-irradiation (n=3-5 biological replicates, Student's t-test at $P < 0.05$*).

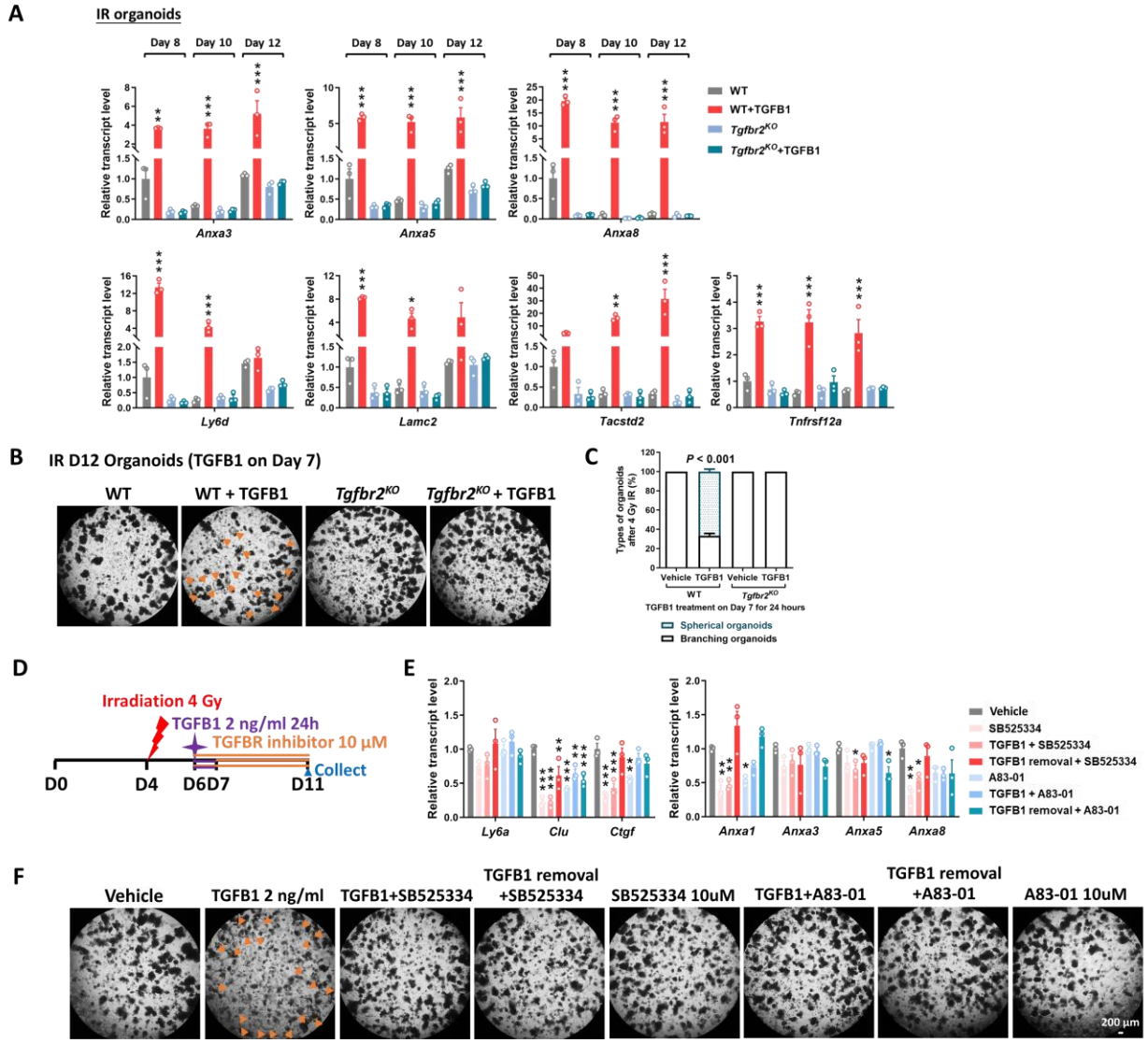

Figure S4. Inactivation of *Tgfbr2* abolishes TGFB1-induced spheroid morphology and fetal/regenerative gene signatures. (A) qRT-PCR indicates that expression of regeneration marker genes increases within 24 hours and remains elevated for at least 5 days post-TGFB1 treatment in organoids post-irradiation. This induction is dependent on *Tgfbr2*. Schematic of experimental design of qRT-PCR for panel A is depicted in **Figure 4F**. Transcript levels are relative to WT, and statistical comparisons were performed using one-way ANOVA followed by Dunnett's post at $P < 0.001$***, $P < 0.01$** or $P < 0.05$* (n=3 independent organoid cultures). **(B-C)** Loss of *Tgfbr2* abolishes TGFB1 induced spheroid morphology (orange arrows, n=3 independent organoid cultures). **(B)** Representative images. **(C)** Quantification. Statistical comparisons were performed using one-way ANOVA followed by Dunnett's post at $P < 0.001$. Schematic of experimental design for panels B-C is in **Figure 4F**. These findings were corroborated by adding TGFB receptor inhibitors **(D-F)**. **(D)** Schematic of intervention experiment using TGFB receptor inhibitors. Primary intestinal organoids were exposed to 4 Gy of irradiation on Day 4, followed by TGFB1 treatment (2 ng/ml) on Day 6 for 24 hours. TGFB receptor inhibitor, 10 µM SB525334 or A83-01, was added at the same time with TGFB1 treatment, or added after removal of TGFB1, or

added without TGFB1 pre-treatment. The corresponding intervention continued until Day 11. Organoids were imaged on Day 11, and then collected for qRT-PCR. **(E)** Presence of TGFB receptor inhibitors suppresses TGFB1-induced expression of fetal/regenerative genes. Transcript levels relative to vehicle, and statistical comparisons were performed using one-way ANOVA followed by Dunnett's post at $P < 0.001$***, $P < 0.01$** or $P < 0.05$* (n=3 independent organoid cultures). All the qRT-PCR data are presented as mean ± SEM. **(F)** TGFB receptor inhibitors abolish TGFB1-induced spheroid morphology (orange arrows, n=3 independent organoid cultures).

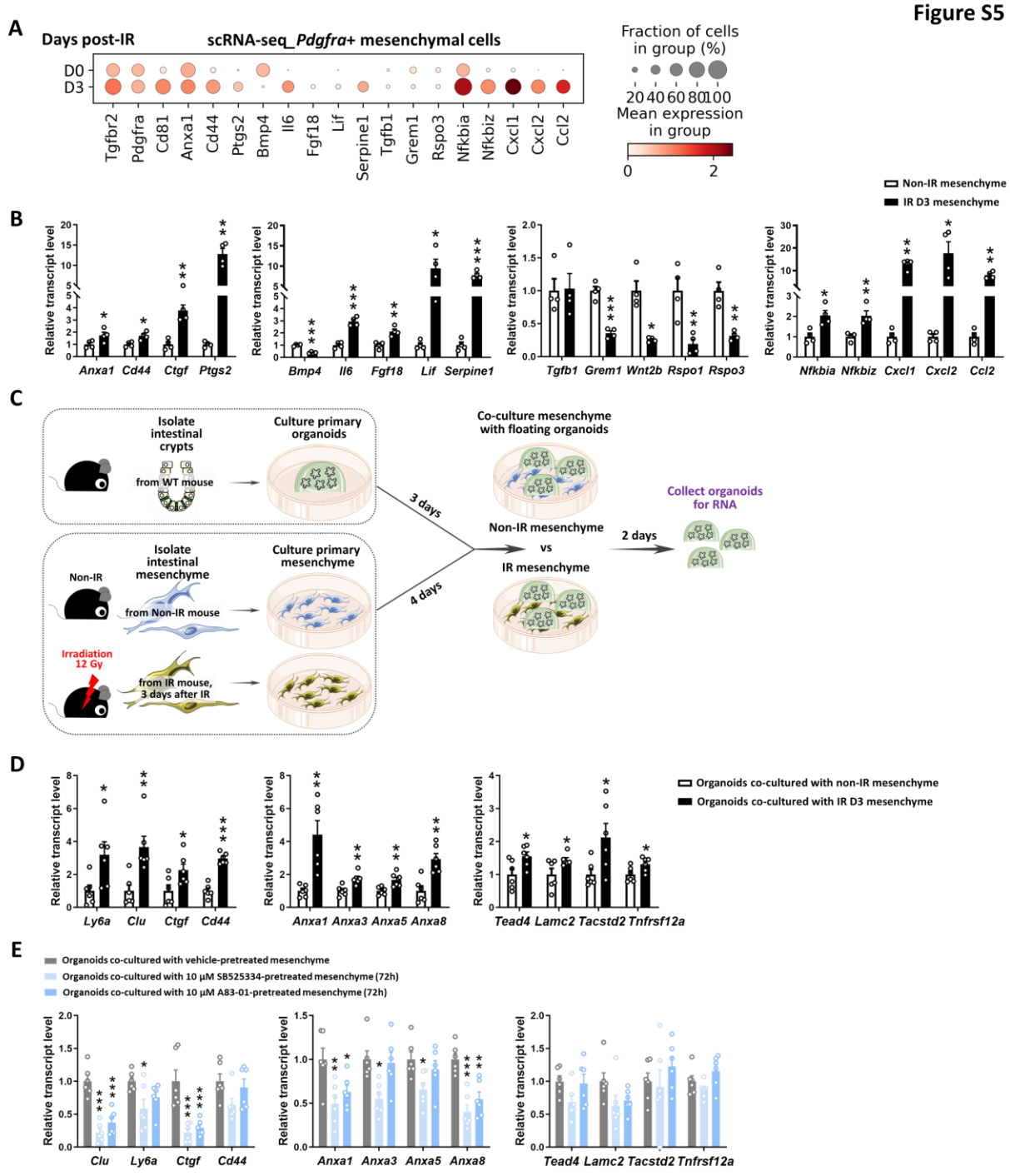

Figure S5. Mesenchyme isolated from mice post-irradiation promotes fetal-like gene signatures of intestinal organoids. (A-B) Cultured mesenchymal cells isolated from mice with or without irradiation harbor similar features of cells isolated from primary *Pdgfra* positive mesenchymal cells, as evidenced by scRNA-seq dot plots **(A)** of *Pdgfra* positive mesenchyme cell cluster (primary cells, GSE165318) and qRT-PCR **(B)** of cultured mesenchyme (n=4 independent mesenchyme cultures with 2 different primary cell lines). **(C)** Schematic of co-culture experimental design. Intestinal mesenchymal cells were isolated from mice with or without irradiation (12 Gy, 3 days post-IR) and cultured for 4 days. They were then overlaid

with Day 3 primary organoids in matrigel bubbles for another 2 days. Co-cultured organoids were collected as floating matrix bubbles for qRT-PCR. **(D)** qRT-PCR reveals that compared to the non-IR condition, mesenchyme isolated from mice post-irradiation shows stronger induction of fetal/regenerative gene expression in co-cultured organoids (n=6 independent organoid cultures with 2 different cell lines of mesenchyme and 3 different cell densities). The qRT-PCR data are presented as mean ± SEM (Student's t-test at $P < 0.001$***, $P < 0.01$** or $P < 0.05$* for panels B and D). **(E)** Mesenchyme pre-treated with TGFBR inhibitors suppresses fetal-like gene signatures of co-cultured intestinal organoids. Passaged intestinal mesenchyme cells were pre-treated with vehicle or TGFBR inhibitors for 3 days, and then co-cultured with Day 3 primary organoids for 2 days (similar procedure as shown in **Figure 5D**). Co-cultured organoids were collected for qRT-PCR (n=6 independent organoid cultures with 2 different cell densities of mesenchyme). TGFBR inhibitors were removed during co-culture. Transcript levels relative to vehicle control, and statistical comparisons were performed using one-way ANOVA followed by Dunnett's post at $P < 0.001$***, $P < 0.01$** or $P < 0.05$*.

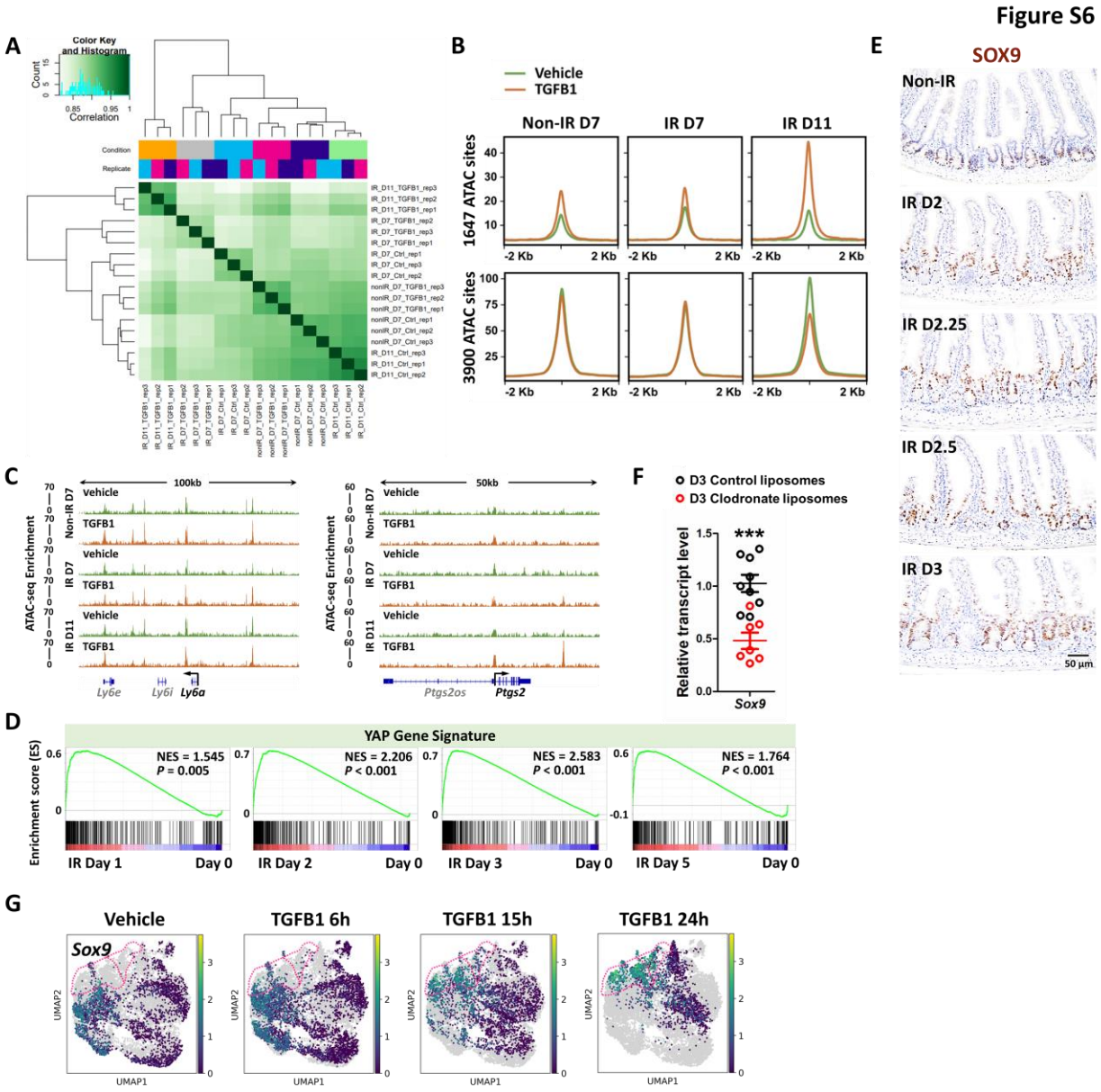

Figure S6. TGFB1 activates intestinal YAP and SOX9 regenerative programs. (A) ATAC-seq correlation heatmap of organoids upon TGFB1 treatment (DiffBind package, n=3 independent organoid cultures, at MACS2 called peaks of q < 0.05). The experimental design is the same as bulk RNA-seq and shown in **Figure 4A**. **(B)** Average signal of ATAC-seq in accessible chromatin regions of vehicle or TGFB1 treated organoids (Differential ATAC-seq regions defined in **Figure 6A**, Diffbind FDR < 0.01). **(C)** Examples of genes located at ATAC-seq enriched regions of TGFB1-treated organoids using IGV. **(D)** GSEA reveals gene signatures of elevated YAP signaling (Gregorieff et al., 2015) post-irradiation, using a bulk RNA-seq of an IR time-course data set (GSE165157 (Qu et al., 2021), crypt cells, n=2 biological replicates per time-course, Kolmogorov-Smirnov test). **(E)** Intestinal immunostaining of SOX9 from day 2 to day 3 post-IR vs. non-IR (brown color; representative of 3 biological replicates). **(F)** Depletion of monocytes/macrophages (main cell sources of TGFB1 secretion) results in a downregulation of *Sox9*, as evidenced by qRT-PCR (n=7-9 biological replicates, duodenal fragments, Student's t-test at $P < 0.001$***). **(G)** scRNA-seq UMAP

plots indicate that TGFB1 induces *Clu*-expressing cells that highly express *Sox9* (shown within pink dotted line, defined in **Figure 4K**). Number of cells in each condition was Vehicle: n= 2815; TGFB1 6h: n= 4071; TGFB1 15h: n= 2788; TGFB1 24h: n=2177.

Figure S7

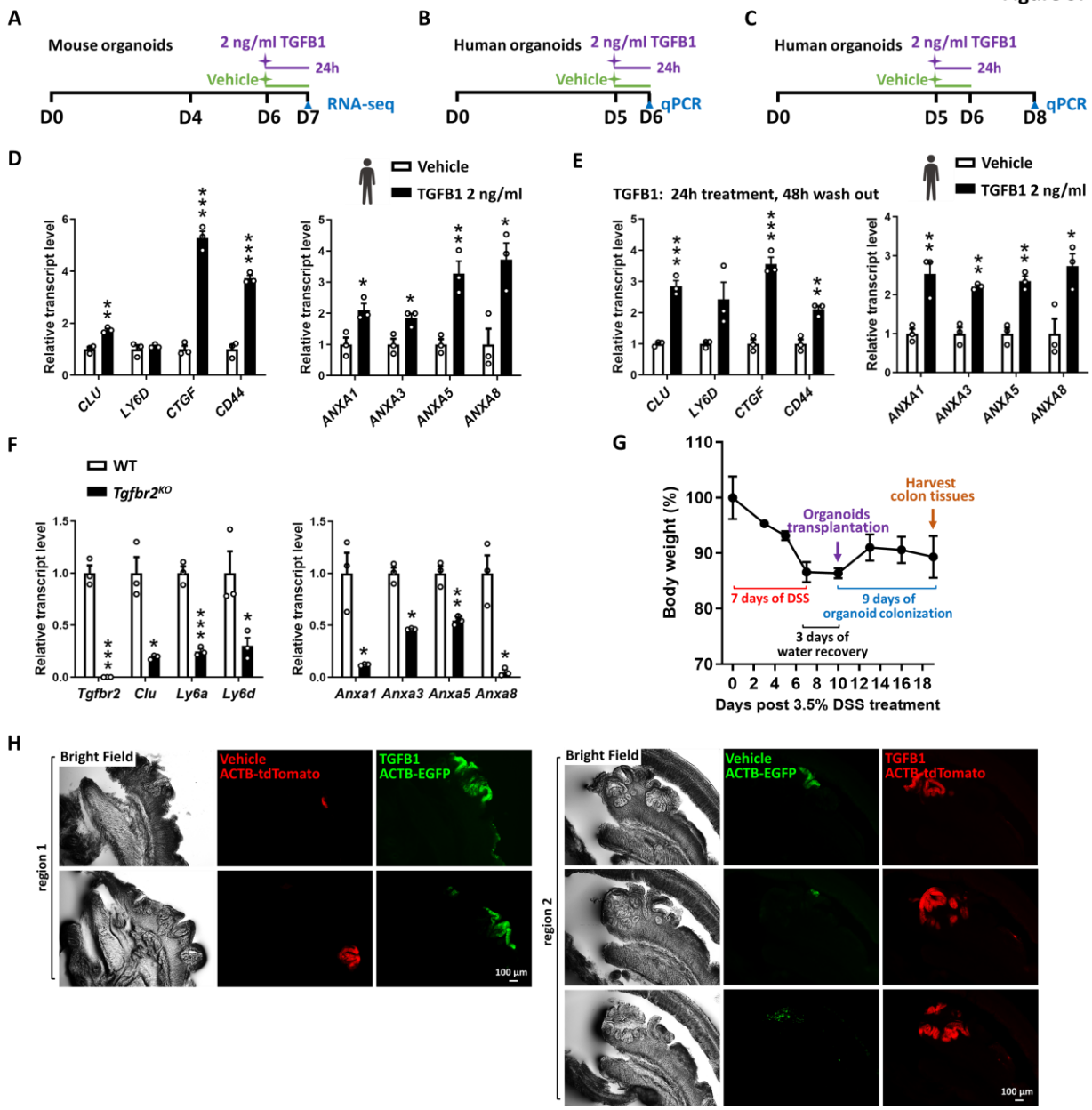

Figure S7. TGFB1 pre-treated organoids transplant more efficiently in DSS-damaged colon. (A) Schematic for the bulk RNA-seq experimental design of non-IR mouse organoids. **(B-E)** TGFB1-induced fetal/regenerative gene signatures are conserved in adult human duodenal organoid cultures. qRT-PCR indicates that expression of regeneration marker genes increases and remains elevated for at least 3 days post-TGFB1-treatment in adult human duodenal organoid cultures. TGFB1 treatment was performed for a 24-hour window either **(B, D)** 24 hours or **(C, E)** 72 hours before collection of cells. Human organoids were treated with TGFB1 on Day 5 (n=3 independent organoid cultures, Student's t-test at $P < 0.001$***, $P < 0.01$** or $P < 0.05$*). All the qRT-PCR data are presented as mean ± SEM. **(F)** To inactivate*Tgfbr2*, *Tgfbr2f/f*; *Villin-Cre*^{ERT2} mice were injected with tamoxifen for 4 consecutive days, and harvested 4 days after the first injection for primary organoid culture. Littermate controls were injected with vehicle. WT and *Tgfbr2*^{KO} organoids were collected on Day 7. qRT-PCR reveals that

fetal/regenerative genes are suppressed in intestinal organoids upon loss of *Tgfbr2* (n=3 independent organoid cultures, Student's t-test at $P < 0.001$***, $P < 0.01$** or $P < 0.05$*). **(G)** Body weight of mice treated with DSS in organoid transplantation experiment. NOD mice were treated with 3.5% DSS for 7 days. After 3 days of water recovery, organoid transplantation was performed and colon tissues were harvested 9 days after organoid transplant (n=5 biological replicates). **(H)** TGFB1 pre-treatment enhances organoid engraftment in DSS-treated mice. Examples of representative regions. Consecutive cryosections that represent the same colonization event were counted as one region. 21 organoid-colonized regions were found from 5 mice.